Silicon (2023) 15:7057–7067
https://doi.org/10.1007/s12633-023-02571-8

RESEARCH

Study on a New Type of Composite Carbon Reducing Agent Pellet with Added Silica

Xiaoyue Wang[1,2] · Zhengjie Chen[1,2,3] · Wenhui Ma[1,2,3] · Jianhua Wen[1,2] · Xiaowei Gan[2,3] · Zicheng Li[3]

Received: 21 April 2023 / Accepted: 16 June 2023 / Published online: 21 June 2023

Abstract

Non-coking coal (NC) and petroleum coke (PC) were mixed in different ratios, and then silica (HBS) with different particle sizes was added to the mixture. Composite carbonaceous reducing agent pellets were prepared by cold pressing. The particle size of raw materials was divided into 80–100 mesh (81MR) and 100–200 mesh (12MR). The effects of four kinds of silica particle size ranges, 40–80 mesh (48 M), 80–100 mesh (81 M), 100–200 mesh (12 M), > 200 mesh (20 M), silica contents 0–5%, and molding pressures 5–25 MPa on the cold strength of pellets with different particle sizes were studied. The optimal processing conditions were a forming pressure of 20 MPa, powder particle size of 12MR, and NC: PC ratio of 7: 3. The addition of 2% of 12 M silica increased the pellet strength to over 9 MPa. The morphology and structure of different carbon materials were characterized by FESEM, FTIR, XPS, and XRD. The results showed that the reason for the difference in pellet performance was the degree of occlusion of the internal particle size of the pellets, and the amounts of surface functional groups and graphitization.

Keywords Industrial silicon · Compound reducing agent · Powder particle size · Compressive strength · Forming mechanism

1 Introduction

As the world's largest renewable energy market and equipment manufacturing country, China's photovoltaic power generation technology is rapidly progressing. More than 80% of the solar cells used in terrestrial photovoltaic systems are made using silicon as the substrate [1, 2]. Polycrystalline silicon accounts for more than 90% of the silicon production of global photovoltaic enterprises [3]. Industrial silicon is at the top of the silicon-based new material industry chain and is the core raw material for the development of "silicon energy" industry chains such as semiconductor materials, organic silicon, aluminum–silicon alloys, and photovoltaics [4]. It has been widely used in the photovoltaic and electronic industries [5–7], as well as aerospace and optical fiber communication applications.

Industrial silicon is produced by placing silica and carbon materials in a submerged arc furnace, inserting three-phase electrodes for submerged arc operation, generating a high temperature (> 1800° C) from the arc, and preparing the metal by carbothermal reduction melting [8–10]. Carbonaceous reducing agents are an essential component of industrial silicon smelting, accounting for 25–30% of production costs [11]. To ensure smooth furnace conditions, high production, and low consumption, the carbon reducing agent must have a high fixed carbon content, low ash content, high resistivity, active chemical properties, low graphitization at high temperatures, and a suitable particle size and mechanical strength [12]. Charcoal meets all of these selection principles [13, 14], but acquiring charcoal requires a large amount of forest resources, which may violate environmental protection laws and exacerbate the greenhouse effect [15]. The limited sources of charcoal make it

✉ Zhengjie Chen
czjkmust@126.com

1 Faculty of Metallurgical and Energy Engineering, Kunming University of Science and Technology, Kunming 650093, China

2 State Key Laboratory of Complex Nonferrous Metal Resources Cleaning Utilization in Yunnan Province, Kunming University of Science and Technology, Kunming 650093, China

3 The National Engineering Laboratory for Vacuum Metallurgy, Kunming University of Science and Technology, Kunming 650093, China

expensive, which increases production costs. Exploring new reducing agents to replace charcoal has become a difficult problem for industrial silicon production [15].

After the United States, China has become the world's largest energy producer and consumer [16, 17]. Because China is coal-rich and contains fewer oil and gas reserves, coal still occupies the leading position in China's energy resources [18–21]. Therefore, it is important to apply coal to the field of industrial silicon smelting. Most relevant research has focused on the reaction characteristics of middling coal during the co-pyrolysis of coal and different biomass materials [22, 23]. Cao et al. [24] combined thermal analysis and kinetics to evaluate the impact of coal and biomass on the carbothermal reduction of silica under different grinding media. They found that different grinding media strongly affected the synergistic effect of biomass and coal, which has important theoretical significance for the comprehensive utilization of coal and biomass to improve the carbothermal reduction of silica. Zhang et al. [25] used a mixture of moldy and fermented biomass and bituminous coal to strengthen the carbothermal reduction of silica and save energy. Zhou et al. [26] used organic solvents as a reaction medium to improve the reactivity of a mixed carbon material (waste fruit peel and coal), which was used as a renewable carbon reducing agent during silicon production. Zhang et al. [27] applied a mixed carbon material of distiller grains and bituminous coal to the carbothermal reduction of silica. They found that the addition of distiller grains increased the chemical reaction rate and lowered the pyrolysis temperature. Considering reducing the cost of the reducing agent and decreasing the waste of powder, here we explore a new type of composite carbonaceous reducing agent to apply non-coking coal during the production of industrial silicon.

In this work, we prepared a new type of composite carbon reducing agent pellet with added silica using non-coking coal as the main raw material. The effects of the silica particle size, silica content, forming pressure, and raw material particle size on the strength of the formed pellets were studied. The morphology and structure of different carbon materials were characterized by FESEM, FTIR, XPS, and XRD spectroscopy. The forming mechanism of pellets under different raw material ratios was analyzed. The pellet strength of the new carbon reducing agent pellet was far greater than the pellet strength required for industrial silicon production by 2 MPa, which can be used in industrial production. This process was conducive to the clean and efficient utilization of low-rank coal and provided great economic and social benefits.

Table 2 Major chemical composition and content of silica (wt.%)

	SiO_2	Al_2O_3	Fe	CaO
HBS	97.71	0.83	0.42	0.077

2 Materials and Experiment

2.1 Materials and Analysis

Non-coking coal (NC) from Xinjiang Province, China was used. An NJ3 bond index tester was used to determine the coking index of 0, and the purchase cost was low. Petroleum coke (PC) was derived from Yunnan Province, China, and silica (HBS) was obtained from Hubei Province, China. The binder (BDO) was a commercially-available organic binder. Table 1 shows the proximate analysis and ultimate analysis of the raw materials PC, NC, and BDO. Table 2 shows the chemical composition and content analysis of the silica.

2.2 Sample Preparation

The preparation flow chart of composite carbonaceous reductant pellets is shown in Fig. 1. The raw materials were carbon materials with different NC: PC ratios (100: 0, 70: 30, 60: 40, and 0: 100) and two particle size ranges (80–100 mesh and 100–200 mesh). To facilitate the distinction, the name 80–100 mesh carbon raw material was defined as 81MR, and 100–200 mesh carbon raw material was 12MR. Four kinds of silica with different particle sizes were added: 40–80 mesh (48 M), 80–100 mesh (81 M), 100–200 mesh (12 M), and > 200 mesh (20 M).

Pellet preparation. First, silica was added to the carbon material and mixed evenly. After mixing with 5% binder and 10% deionized water and stirring well, it was placed in a mold. Then, the mold was placed on a hydraulic press, and the material was pressed by shaking the handle to press the mold. The formed composite pellets were cylinders with a diameter of 25 mm and a height of 13–15 mm. Finally, the formed pellets were placed in a drying oven at 80 °C for 4 h and cooled to room temperature to obtain composite carbonaceous reducing agent pellets. Three samples were

Table 1 Proximate and ultimate analysis of raw materials (wt.%)

	Proximate analysis				Ultimate analysis				
	FC	V	M	A	C	H	O	N	S
PC	89.105	10.69	0.18	0.025	90.71	1.48	1.14	1.54	2.94
NC	60.37	32.97	2.49	4.17	72.72	3.91	15.70	0.42	0.16
BDO	2.65	89.88	7.37	0.10	38.49	5.47	46.54	0.21	—

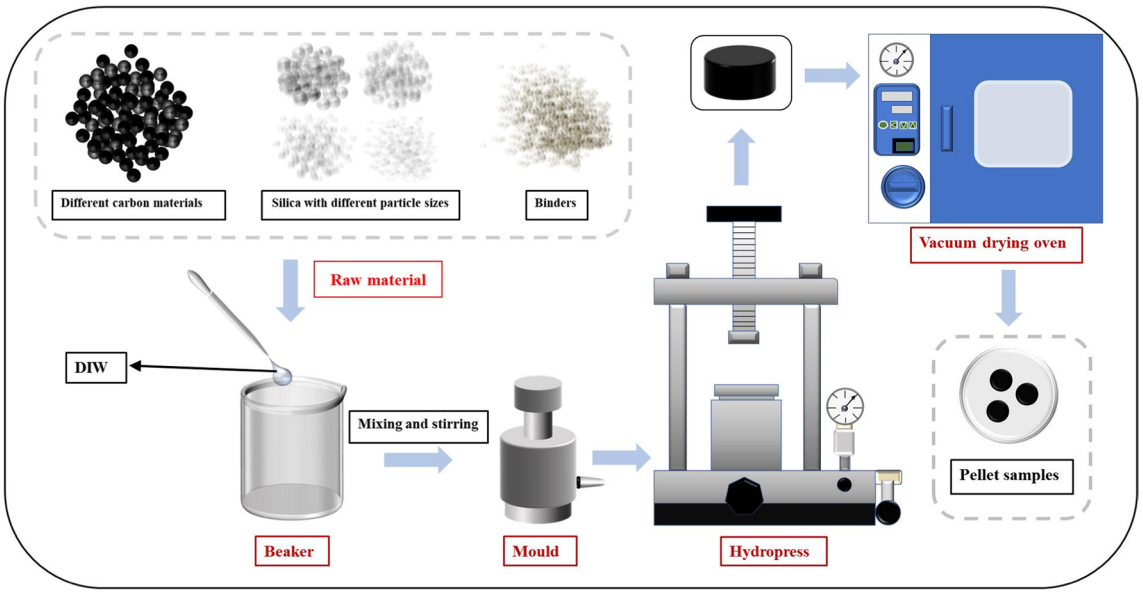

Fig. 1 Flow chart for the preparation of new composite carbon reducing agent pellets

prepared for each type of pellet. The cold strength of pellets was tested by an LXM-8000 cold strength tester, and the compressive strength was calculated from the average.

A certain quality of non-coking coal and petroleum coke were taken, respectively. To test the forming mechanism of different carbon materials, we used a field emission scanning electron microscope (Nova NanoSEM 450) to analyze the morphology and structure of the samples. The functional groups and chemical structures of different carbon materials were analyzed by a Bruker ALPHA infrared spectrometer, scanning XPS Microprobe system (PHI5000 Versaprobe-II), and an X-ray diffractometer (D / Max-2200). The field emission scanning electron microscope had a high stability and ultra-high resolution, a Schottky field emission electron gun with high-vacuum and low-vacuum modes (< 200 Pa). The magnification range was 30–1 000 000 times, the acceleration voltage was 200 V – 30 kV, and the electron beam current range was 0.3 pA – 100 nA. The ALPHA infrared spectrometer had a spectral range of 4000–400 cm^{-1}, 16 scans, and a spectral resolution of 4 cm^{-1}. The XPS microprobe system operated at a power of 50 W, a voltage of 15 kV, an Al rake anode, and a pass energy of 46.95 eV. The X-ray diffractometer used Cu-K_α as the radiation source ($\lambda = 0.15406$ nm). The working voltage was 40 kV, the working current was 40 mA, the scanning speed was 3°/min, and the scanning range was 10–90°.

3 Results and Discussion

3.1 Effect of Particle Size (Carbon Raw Materials and Silica) on Pellet Strength

The raw materials were 81MR and 12MR with different ratios, the silica content was 3%, the forming pressure was 20 MPa, and the silica particle size was the single variable in the experiment.

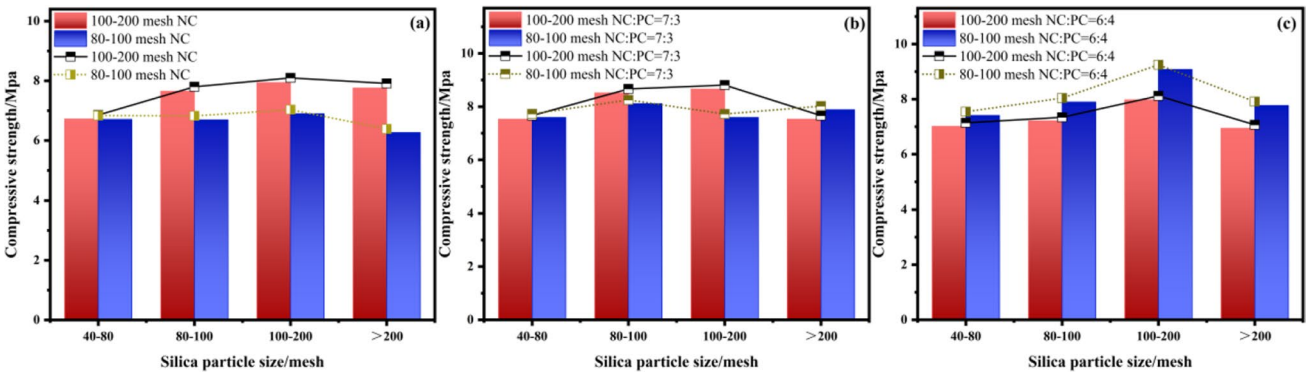

Fig. 2 The effect of (48 M, 81 M, 12 M, 20 M) silica on the compressive strength of 81MR and 12MR pellets. (**a**) The raw material is NC. (**b**) The raw material is NC : PC = 7 : 3. (**c**) The raw material is NC : PC = 6 : 4

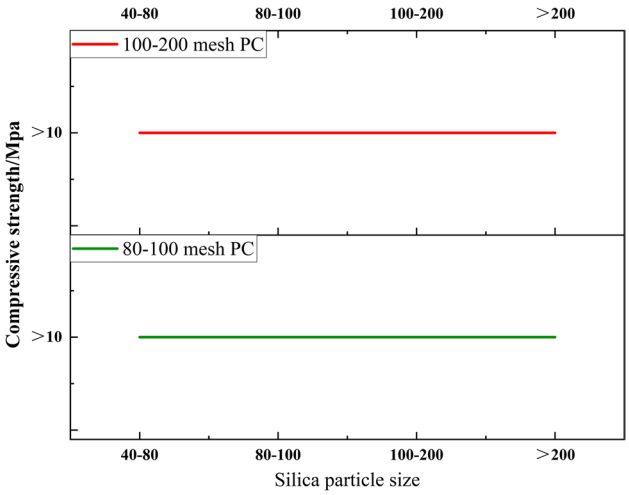

Fig. 3 Effects of adding different particle sizes (48 M, 81 M, 12 M, 20 M) of silica on the compressive strength of petroleum coke pellets

The effect of adding different silica particle sizes (48 M, 81 M, 12 M, 20 M) on the compressive strength of the pellets is shown in Fig. 2. The compressive strength of pellets of 12MR and 81MR was significantly different, and the strength of the sample with 12 M silica pellets was higher. Figure 2a and b show that the compressive strength of 12MR pellets was better than that of 81MR. The specific differences between 12 and 81MR pellets were as follows: (1) When the raw material was 81MR, the strength of non-coking coal pellets was maintained in the range of 6.5–7 MPa. The compressive strength of pellets increased significantly when petroleum coke was added to non-coking coal. When 30% petroleum coke was added, the pellet strength increased to 7.5–8.5 MPa. When 40% petroleum coke was added, the strength was 7.5–9 MPa. When 12 M silica was added, the maximum pellet strength exceeded 9 MPa. (2) When the raw material was 12MR, the strength of non-coking coal pellets remained in the range of 6.7–8 MPa. When adding 30% PC, the pellet strength increased to 7.5–8.7 MPa. When 40% PC was added, the strength of pellets was not improved, and the strength was smaller than that of non-coking coal pellets. This was the opposite result from when the particle size was 81MR. The reason for this result was likely related to the structural properties of the raw materials.

Figure 3 shows the effect of adding (48 M, 81 M, 12 M, 20 M) silica on the compressive strength of petroleum coke pellets. When the particle size of silica was a single variable in the experiment, the compressive strength of 81MR and 12MR petroleum coke pellets was greater than 10 MPa, which exceeds the equipment range. Whether the specific addition of silica is the main reason for the high strength requires exploring the influence of different silica contents on the compressive strength of petroleum coke pellets.

3.2 Effect of Silica Content on Pellet Strength

The raw materials were 81MR and 12MR with different ratios, silica was 12 M, the forming pressure was 20 MPa, and the silica content was the single variable in this section's experiment.

Figure 4 shows the effect of adding different contents of 12 M silica on the compressive strength of pellets. When different silica contents were added to the 81MR, the strength of the coal pellets in non-coking remained in the range of 6.5–7 MPa. The strength of pellets containing 30% petroleum coke was maintained in the range of 6.5–8.5 MPa. When 40% petroleum coke and 3% silica were added, the strength reached the maximum value of 9.081 MPa. The raw material was 12MR, and the difference between pellet strength was obvious. When the content of petroleum coke was 30%, the strength of pellets was effectively improved upon increasing the silica content. When the silica content was 2%, the pellet strength reached a maximum of 9.098 MPa. When the petroleum coke content was 40%, the pellet strength was less than that of the non-coking coal pellets, which was opposite to the experimental results of

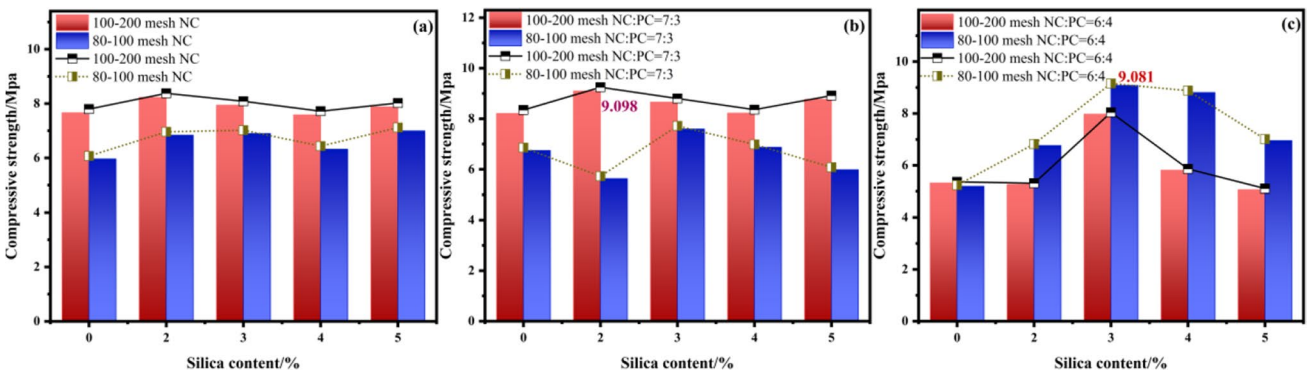

Fig. 4 Effects of different contents of 12 M silica on the compressive strength of 81MR and 12MR pellets. (**a**) The raw material is NC. (**b**) The raw material is NC : PC = 7 : 3. (**c**) The rawmaterial is NC : PC = 6 : 4

81MR. Overall, when the raw material was 81MR, adding 3% 12 M silica content produced stronger pellets. When the raw material was 12MR, adding 2% 12 M silica provided the strongest pellets.

Figure 5 shows the effect of adding 81 M and 12 M silica on the compressive strength of 81MR NC: PC = 7: 3 pellets. When the raw material was 81MR, adding PC30% and 81 M silica 3% produced pellets with the maximum strength. Figure 2b shows that when the raw material was 81MR NC: PC = 7: 3, the strength of the added 81 M silica pellets reached the maximum. Therefore, we measured the effect of adding different 81 M silica contents on the compressive strength of 81MR pellets with a PC content of 30%. We then compared this to the experimental results of adding different 12 M silica contents. Figure 5 shows that the strength of pellets with 81 M silica was much higher. When the silica content was 2%, the strength of pellets containing 81 M silica was 14% higher than that of pellets containing 12 M silica.

Figure 6 shows the effect of adding different contents of 12 M silica on the compressive strength of petroleum coke pellets. When the silica content was 0, the strength was greater than 10 MPa, showing that the strength increase was independent of silica. The main reason might be that petroleum coke is easily-graphitized carbon [28]. The microcrystalline carbon grid flakes of petroleum coke overlap neatly, and the distance between the flakes is small. It is a highly aromatized polymer carbide [29]. This structure gives the petroleum coke particles a certain hardness that is conducive to the close combination of water and binder with the material, which promotes press molding.

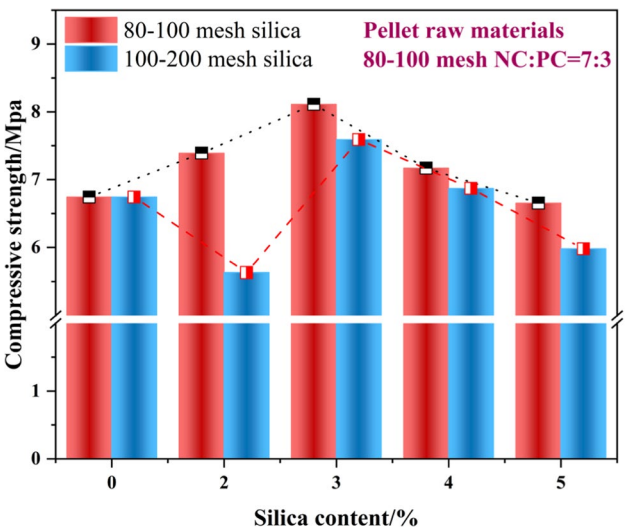

Fig. 5 Effects of adding different contents of 81 M and 12 M silica on the compressive strength of 81MR NC:PC = 7: 3 pellets

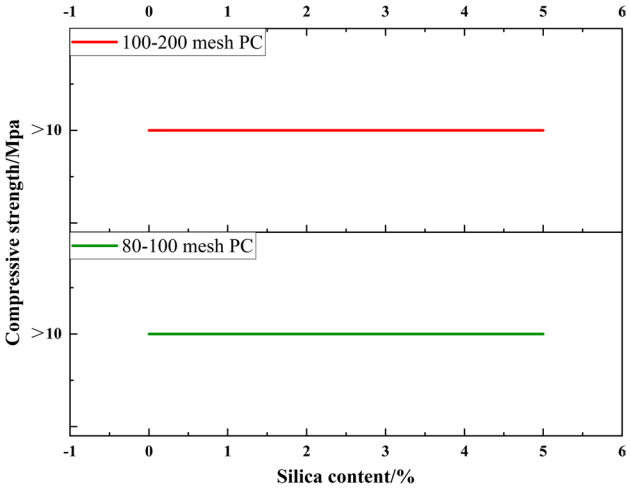

Fig. 6 Effect of adding different content of 12 M silica on the compressive strength of petroleum coke pellets

3.3 Effect of Forming Pressure on Pellet Strength

The raw materials were 81MR and 12MR with different ratios, 3% 12 M silica was added, and the forming pressure was the single variable in the experiment in this section.

Figure 7a and b are the effects of forming pressure on the compressive strength of 81MR and 12MR pellets, respectively. As the forming pressure increased, the pellet strength gradually increased and began to decrease after reaching the maximum at 20 MPa. Under the action of forming pressure, gases between the particles were gradually discharged, which destroyed the arch bridge effect of the material, rearranged the particles inside the agglomerate, and gradually densified to form a pellet. Internal friction between the particles affected their approach, making the strength of the pellet increase slowly. When the pressure was greater than a certain value, the larger particles underwent secondary fragmentation, increasing the new section because there was no binder at fracture locations. Therefore, the surface of the pellet produced more cracks, which decreased the strength of the pellet.

Figure 8 shows the effect of forming pressure on the compressive strength of pellets with different particle sizes (12MR and 81MR). The strength of 12MR pellets was greater than that of 81MR pellets under different pressures. This was because when using 100–200 mesh particles, the surface contact between the powder particles was good, and the particles and silica were intertwined and filled each other, providing a high filling density. This decreased the compression ratio, thus increasing the pellet strength.

Figure 9 shows the effect of forming pressure on the compressive strength of petroleum coke pellets. When the pressure was 5 MPa, the compressive strength of

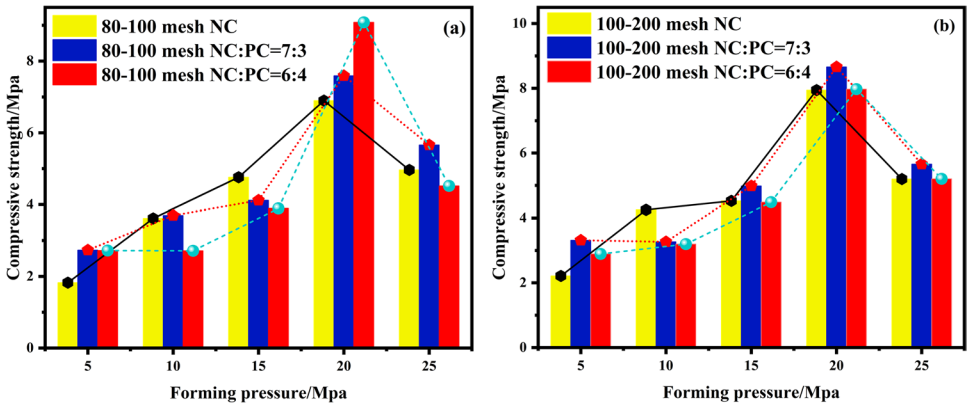

Fig. 7 Effect of forming pressure on the compressive strength of carbon pellets with the same particle size. (**a**) The particle size of the raw material is 80-100 mesh. (**b**) The particle size of rawmaterials is 100-200 mesh

petroleum coke pellets exceeded 10 MPa. It is speculated that petroleum coke contains functional groups that enhance the hydrophilicity, corresponding chemical energy, viscous energy, and capillary attraction energy of the particle surface. The binder chemically adsorbed on particle surfaces, thereby improving the strength of the pellets. The specific reasons will be verified in Section 4.

From the above experimental results, it can be seen that adding petroleum coke to coal and adding a small amount of silica to the carbonaceous reducing agent greatly improved the pellet strength. The content and particle size of silica in pellets should be moderate. If the particle size is too small to fill the pores between the particles, the pellet strength and density will be low. If the particle size is too large, it will lead to difficult movement and deformation during pressing. The number of silica particles exceeded a certain range, which increased the porosity and decreased the mechanical strength. The particle size of the powder had a great influence on the strength of the pellets. The smaller the particles, the larger the specific surface area, the looser the structure, the stronger the adsorption of the binder, and the higher the pellet strength. The experimental results showed that when the forming pressure was 20 MPa and the powder was 12MR NC: PC = 7: 3, pellets with the best performance were obtained by adding 2% silica with a particle size of 12 M.

4 Pellet Forming Mechanism Analysis

4.1 Performance Analysis of Silica

Silicon ore used in the experiment and the structure of SiO_2 [30] are shown in Fig. 10. The silicon ore used in this experiment was composed of 98% SiO_2. Figure 10 shows that silica had a tetrahedral network structure composed of silicon atoms and oxygen atoms, in which silicon atoms were located in the center of the regular tetrahedron, and four oxygen atoms were located at the vertices of the tetrahedron. Each silicon atom formed a Si–Si covalent bond with adjacent silicon atoms, and each two silicon atoms were connected by an oxygen atom. This regular tetrahedral structure formed a solid interconnected spatial network crystal, making silica highly stable and hard. Dense and hard silica was added to the carbon raw material, which improved the

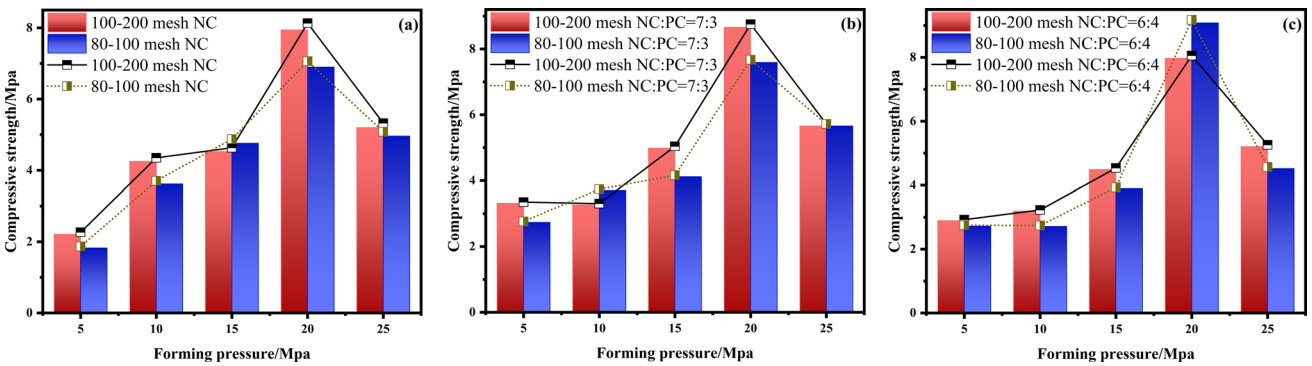

Fig. 8 Effect of forming pressure on compressive strength of pellets with different particle sizes (81MR and 12MR). (**a**) The raw material is NC. (**b**) The raw material is NC : PC = 7 : 3. (**c**) The raw material is NC : PC = 6 : 4

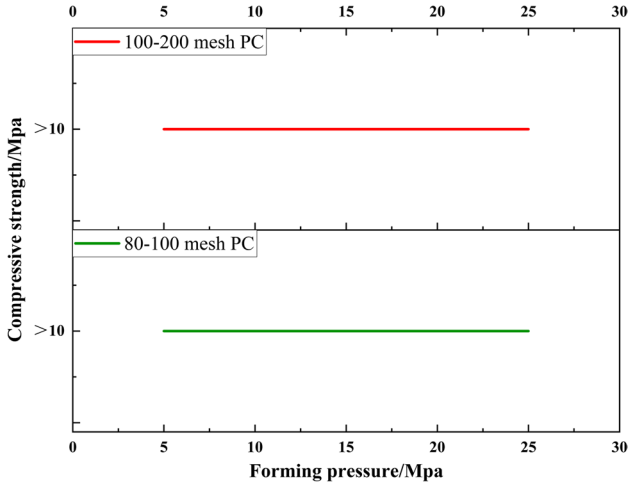

Fig. 9 Effect of forming pressure on compressive strength of petroleum coke pellets

hardness of the material. After the pellet was formed, silica acted as a skeleton in the pellet, giving it superior strength. However, Fig. 4 shows that the optimal silica content was in the range of 0–5% due to the different performance of the carbon materials. Therefore, next we need to analyze the specific structure and functional groups of non-coking coal and petroleum coke.

4.2 FESEM Micrographs

Figure 11 shows the FESEM analysis of NC and PC. The surface of the coal particles in non-coking coal was rough and irregular, with many sharp protrusions and voids. After magnification, the surface cracks were large, and a small number of small particles was attached. The structure was not conducive to the combination of particles during powder pressing, and more binder and water were needed to fill the gap. The surface of petroleum coke was smooth and attached with many small particles, and there were some pores on the surface without cracks. The structure was conducive to the close combination between the material and binder so that the binder was evenly distributed on the surface and pores of the particles. This made it easy to press and mold, and the strength of the petroleum coke pellets also increased.

4.3 FTIR Spectroscopy

The infrared spectra of NC and PC are shown in Fig. 12. Figure 12 show that the functional groups of non-coking coal and petroleum coke were very different, which also led to the difference in the performance of the two after balling. Petroleum coke contains five functional groups, -OH, C=C, C=O, $-CH_2$, and =C-H, while non-coking coal contained only C=C and C=O. The -OH functional group in petroleum coke has similar properties to water and can form hydrogen bonds with water. After adding a certain proportion of water into petroleum coke powder, the hydrophilic substances on the surface of the particles formed a layer of directionally-arranged water molecules on the surface of the particles through the action of permanent dipole and hydrogen bonds, i.e., a hydration film. Water molecules also acted as a reaction medium between the material and the binder, so that the binder was uniformly adsorbed on the surface of the particles. Under a certain forming pressure, the particles were connected by the binder and hydration film. During pellet drying, water continuously evaporated, and the hydration film became thinner, which reduced the particle dispersion, increased the van der Waals forces between molecules, merged and aggregates the petroleum coke particles, and produced a certain mechanical meshing force that further improved the strength of the pellets. Therefore, the strength of petroleum coke pellets in this study was greater than that of non-coking coal pellets and mixed materials (NC and PC) pellets.

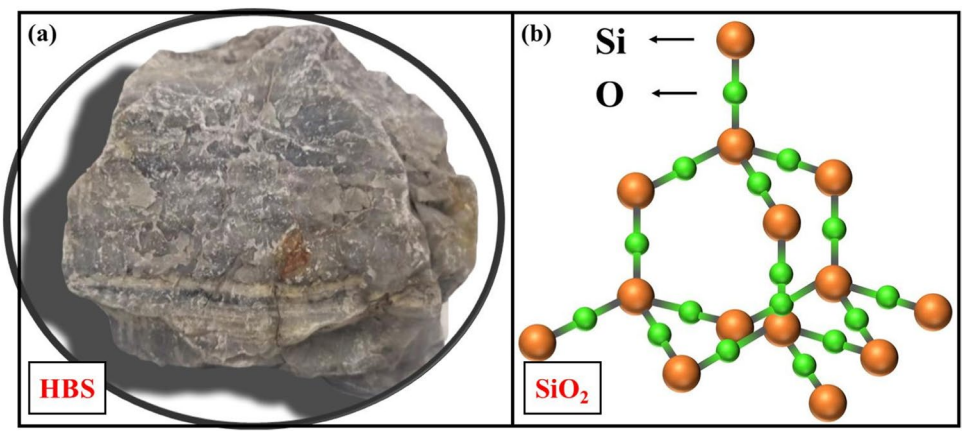

Fig. 10 (**a**) Silicon ore. (**b**) Structure of SiO_2 [30]

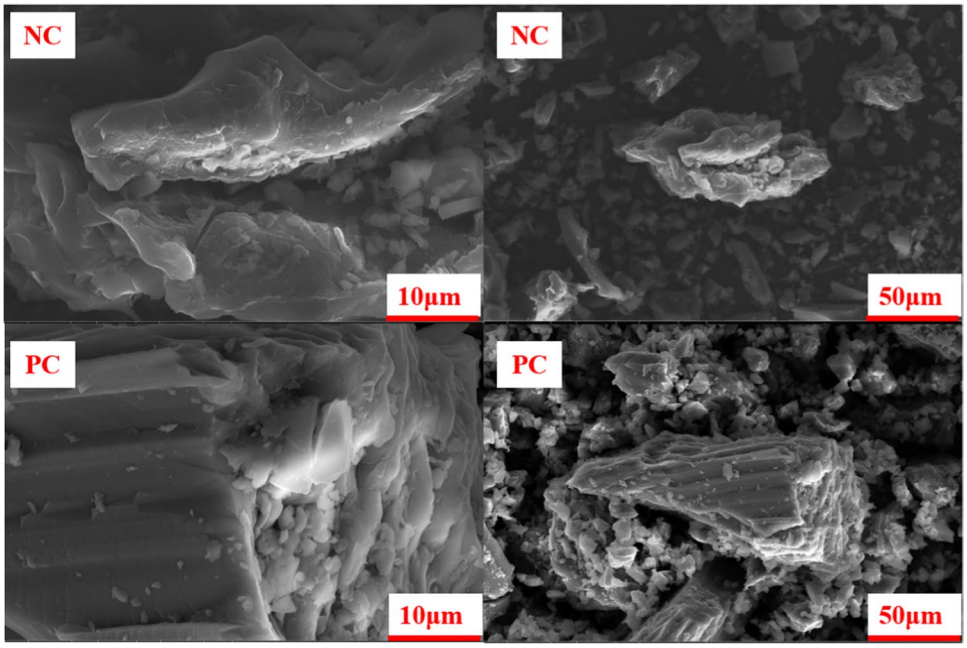

Fig. 11 FESEM images of NC and PC

4.4 XPS Spectroscopy

To further determine the chemical structure of the sample, we conducted XPS analysis on non-coking coal and petroleum coke. Figure 13 is the XPS full spectrum and C 1 s and O 1 s fitted spectra of non-coking coal and petroleum coke. The C 1 s spectra of non-coking coal and petroleum coke show that the two raw samples contained a graphite-like structure. Graphite is a transitional crystal that lies between an atomic crystal, metal crystal, and molecular crystal. The carbon atoms in the same layer of the crystal were sp^2 hybridized to form C = C bonds [31]. Each carbon atom was connected to three other carbon atoms. Six carbon atoms formed a regular hexagonal ring in the same plane and stretch to form a sheet structure [31]. Figure 13 shows that both samples contained carbonyl groups, but only petroleum coke contained polar group hydroxyl groups, which corresponds to the infrared spectra analysis results of the two samples.

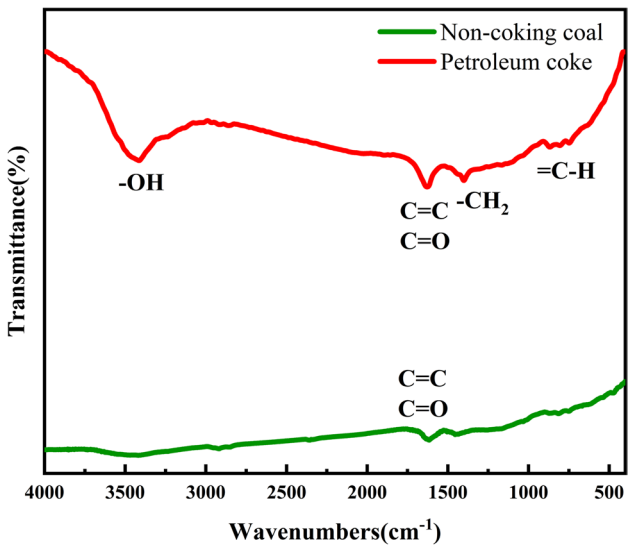

Fig. 12 Infrared spectrum analysis of NC and PC

4.5 XRD Spectroscopy

XRD was performed to explore the relationship between pellet strength, carbon structure, and graphitization degree of different carbon materials. XRD analysis of NC and PC are shown in Fig. 14. According to the XRD pattern characteristics of the graphitization process of carbon materials, the higher the degree of graphitization, the sharper the corresponding peak, called the sharp peak, otherwise called the low peak [32, 33]. The peak shape of petroleum coke was sharper and more symmetrical, indicating a higher graphitization degree. The diffraction peaks corresponding to the (002) crystal planes represented the spatial orientation of the aromatic network structure. The higher the degree of graphitization, the more regular the orientation of the aromatic network, the smaller the d_{002} spacing between aromatic layers, and the narrower the half-peak width. The d_{002} value [34] was calculated by substituting the peak fitting parameters into Eq. 1:

$$d_{002} = \frac{\lambda}{2\mathrm{Sin}\theta} \quad (1)$$

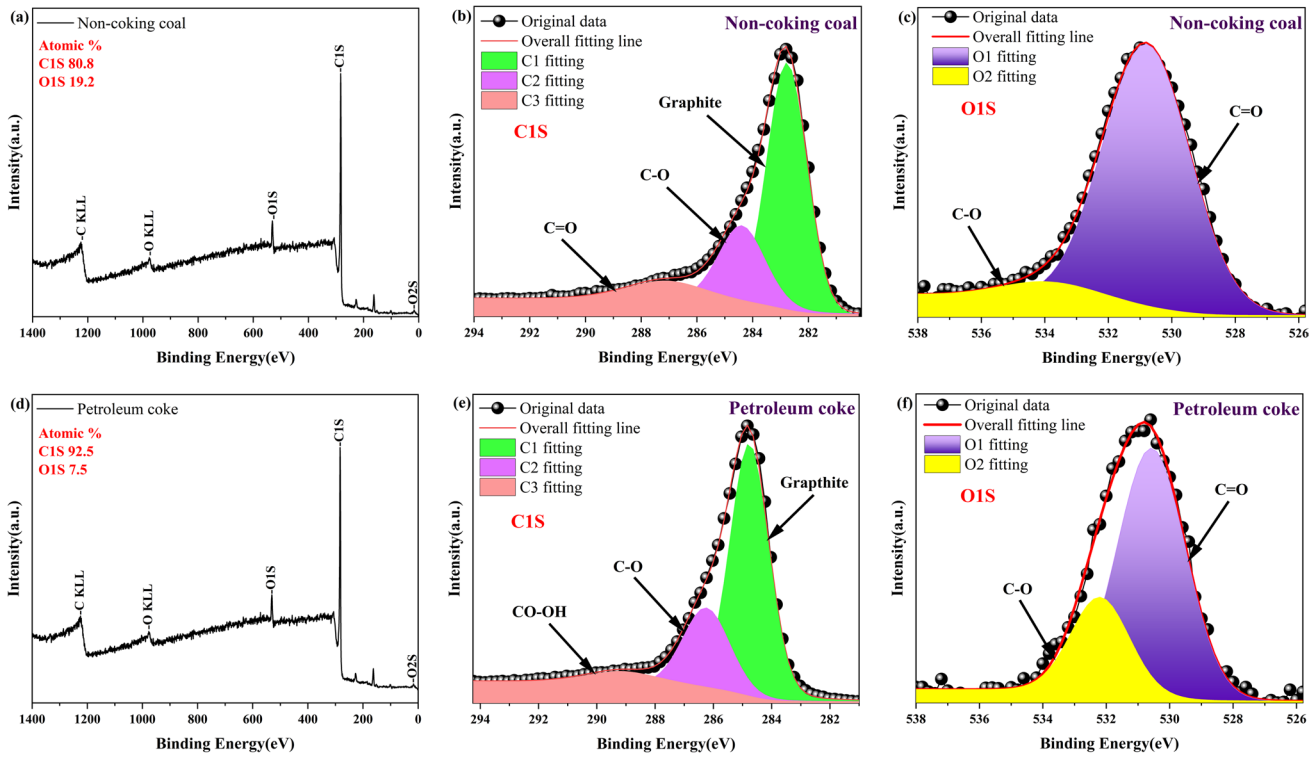

Fig. 13 XPS full spectrum and C1S, O1S spectrum fitting analysis of NC and PC samples

Table 3 lists the fitted peak data and d_{002} values of NC and PC XRD patterns. X_C is the peak weighted average center, FWHM is the full-width at half peak. The FWHM of petroleum coke was smaller, and d_{002} between aromatic layers was smaller and closer to an ideal natural hexagonal graphite structure. The relative density of the structure was small, and the binding between carbon atoms was strong, making it extremely difficult to destroy. After being pressed into pellets, the particles were tightly bonded, and the mechanical strength increased. This result is consistent with the analysis in Section 3.2.

When the raw material was 12MR NC: PC = 6: 4, adding petroleum coke increased the graphite carbon network structure of the material and reduced the hydrophobicity of the powder. These were beneficial to the close combination of the material, but upon decreasing the coal ratio in non-coking coal, the surface voids of the raw materials also decreased. During pressing, the combination of the rough surface of non-coking coal and the smooth surface of petroleum coke was unbalanced, and the particles were not closely bonded to each other. Because of this, the distribution of binder and water was uneven, the density of raw materials was low, and the strength of pellets was reduced.

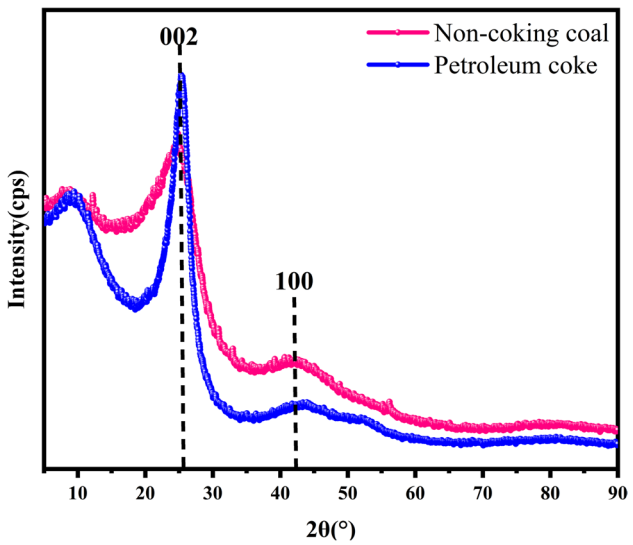

Fig. 14 XRD spectrum analysis of PC in NC

Table 3 Peak fitting parameters of XRD spectra and d_{002} value

Samples	X_C(2θ/°)	FWHM/rad	d_{002}/nm
Non-coking coal	24.88	0.59	0.36
Petroleum coke	25.33	0.40	0.35

5 Conclusion

Using non-caking coal as the main raw material, we prepared composite carbonaceous reducing agent pellets by adding silica. The effects of silica particle size, silica content, and forming pressure on the compressive strength of formed pellets were studied using 81MR and 12MR as raw materials, respectively, using single-factor experiments. The results showed that adding silica to the carbon material and petroleum coke to coal greatly improved the compressive strength of the pellets. The silica particles acted as a skeleton in the agglomerate interior. The surface of the petroleum coke was smooth and porous and contained hydrophilic groups and had a graphitized structure. These factors increased the strength of the pellets after forming. The experimentally-determined optimal process conditions using 12MR NC: PC = 7: 3 as the carbon raw material were added 2% 12 M silica and a forming pressure of 20 MPa. This reducing agent was applied to the carbothermal reduction of SiO_2, which decreased the amount of reducing agents such as charcoal during the production of industrial silicon and reduced the loss of silicon. This paper has guiding significance for the research and applications of composite carbonaceous reducing agents for industrial silicon smelting.

Acknowledgements The authors are grateful for financial support from the Major Projects of Yunnan Province (No. 202102AB080013 and No. 202303AC100006) and the Key Science and Technology Specific Projects of Yunnan Province (No. 202202AG050012).

Authors' Contributions **Xiaoyue Wang:** Conceptualization, Resources, Writing—review & editing, Visualization, Validation, Supervision. **Zhengjie Chen:** Conceptualization, Methodology, Validation, Formal analysis, Investigation, Data curation; **Wenhui Ma:** Formal analysis, Validation, Data curation; **Jianhua Wen:** Conceptualization, Resources; **Xiaowei Gan**: Visualization; **Zicheng Li:** Visualization, Supervision.

Funding The authors are grateful for financial support from the Major Projects of Yunnan Province (No. 202102AB080013 and No. 202303AC100006) and the Key Science and Technology Specific Projects of Yunnan Province (No. 202202AG050012).

Data Availability All data generated or analysed during this study are included in this published article.

Declarations

Ethics Approval and Consent to Participate We don't cover ethics approval and consent to participate.

Consent for Publication Not applicable.

Informed Consent Not applicable.

Research involving Human Participants and/or Animals Not applicable.

Competing Interests The authors declare that they have no competing interests.

References

1. Möller HJ, Funke C, Rinio M, Scholz S (2005) Multicrystalline silicon for solar cells. Thin Solid Films 487(1–2):179–187
2. Saffar S, Abdullah A, Gouttebroze S, Zhang ZL (2014) Ultrasound-assisted handling force reduction during the solar silicon wafers production. Ultrasonics 54(4):1057–1064
3. Flamant G, Kurtcuoglu V, Murray J, Steinfeld A (2006) Purification of metallurgical grade silicon by a solar process. Sol Energy Mater Sol Cells 90(14):2099–2106
4. Kabir E, Kumar P, Kumar S, Adelodun AA, Kim KH (2018) Solar energy: potential and future prospects. Renew Sustain Energy Rev 82:894–900
5. Müller A, Ghosh M, Sonnenschein R, Woditsch P (2006) Silicon for photovoltaic applications. Mater Sci Eng B 134(2–3):257–262
6. Ni Z, Zhou S, Zhao S, Peng W, Yang D, Pi X (2019) Silicon nanocrystals: unfading silicon materials for optoelectronics. Mater Sci Eng R Rep 138:85–117
7. Cristea D, Craciunoiu F, Caldararu M (2000) Components for optoelectronic and photonic integrated circuits—design, modelling, manufacturing and monolithic integration on silicon. Mater Sci Eng, B 74(1–3):89–95
8. Schei A, Tuset JK, Tveit H (1998) Production of high silicon alloys. Tapir, Trondheim, pp 301–315
9. Bisio G, Rubatto G, Martini R (2000) Heat transfer, energy saving and pollution control in UHP electric-arc furnaces. Energy 25(11):1047–1066
10. Dosaj VD, May JB, Arvidson AN (1994) Direct current, closed furnace silicon technology (No. CONF-9406164–1). Dow Corning Corp., Midland
11. Strakhov VM, Surovtseva IV, Elkin DK, Elkin KS, Cherevko AE (2012) Low-ash carbon reducing agents for electrothermal silicon production. Coke Chem 55(5):172–175
12. Wang XY, Chen ZJ, Ma WH, Wen JH (2022) Application of semi-coke in industrial silicon production. Silicon 15:3379–3386
13. Chen ZJ, Zhou SC, Ma WH, Deng XC, Li SY, Ding WM (2018) The effect of the carbonaceous materials properties on the energy consumption of silicon production in the submerged arc furnace. J Clean Prod 191:240–247
14. Chen ZJ, Ma WH, Wei KX, Li SY, Ding WM (2017) Effect of raw materials on the production process of the silicon furnace. J Clean Prod 158:359–366
15. Zhou SC, Chen ZJ, Ma WH, Li SY, Yang X, Cao SJ (2021) Effects of grinding media on the material properties and strengthening mechanism of silicon production. J Clean Prod 278:123438
16 Statistics I E A (2014) Key world energy statistics. International Energy Agency, Paris
17. Gregory J, Stouffer RJ, Molina M, Chidthaisong A, Solomon S, Raga G, Stone D A (2007) Climate change 2007: the physical science basis
18. Niu C, Xia W, Xie G (2017) Effect of low-temperature pyrolysis on surface properties of sub-bituminous coal sample and its relationship to flotation response. Fuel 208:469–475
19. Wang C, He B, Yan L, Pei X, Chen S (2014) Thermodynamic analysis of a low-pressure economizer based waste heat recovery system for a coal-fired power plant. Energy 65:80–90
20. Zhao Y, Feng D, Li B, Wang P, Tan H, Sun S (2019) Effects of flue gases (CO/CO2/SO2/H2O/O2) on NO-Char interaction at high temperatures. Energy 174:519–525
21. Zhang H, Dou B, Li J, Zhao L, Wu K (2020) Thermogravimetric kinetics on catalytic combustion of bituminous coal. J Energy Inst 93(6):2526–2535
22. Wu Z, Meng H, Luo Z, Chen L, Zhao J, Wang S (2017) Performance evaluation on co-gasification of bituminous coal and wheat straw in entrained flow gasification system. Int J Hydrogen Energy 42(30):18884–18893

23. Merdun H, Laougé ZB (2021) Kinetic and thermodynamic analyses during co-pyrolysis of greenhouse wastes and coal by TGA. Renew Energy 163:453–464
24. Cao SJ, Zhou SC, Chen ZJ, Ma WH (2021) Effect of grinding media on the synergistic characteristics of coal and biomass for the carbothermal reduction of silica. Phosphorus Sulfur Silicon Relat Elem 196(6):594–603
25. Zhang HM, Chen ZJ, Ma WH, Cao SJ (2022) Effect of the reactive blend conditions on the thermal properties of waste biomass and soft coal as a reducing agent for silicon production. Renew Energy 187:302–319
26. Zhou SC, Chen ZJ, Yin G, Ma WH, Cao S (2021) Influence of the grinding media applying in the soft coal and waste biomass on the carbothermic reduction process of silica. Silicon 13:3963–3970
27. Chen ZJ, Zhang HM, Ma WH, Wu JJ (2022) High efficient and clean utilization of coal for the carbothermic reduction of silica. Sustain Energy Technol Assess 53:102602
28. Zhan X, Zhou Z, Wang F (2010) Catalytic effect of black liquor on the gasification reactivity of petroleum coke. Appl Energy 87(5):1710–1715
29. Bayram A, Müezzinoğlu A, Seyfioğlu R (1999) Presence and control of polycyclic aromatic hydrocarbons in petroleum coke drying and calcination plants. Fuel Process Technol 60(2):111–118
30. Materials Project (n.d.) Retrieved [2023.5.18], from https://materialsproject.org/
31. Mills BF (1942) Porosity and oil absorption properties of metal compacts of copper-tin-graphite. Digital Commons @ Montana Tech. https://digitalcommons.mtech.edu/bach_theses/166/
32. Chen ZJ, Ma WH, Wei KX, Wu JJ, Li SY, Zhang C, Yu J (2017) Detailed vacuum-assisted desulfurization of high-sulfur petroleum coke. Sep Purif Technol 175:115–121
33. Li W, Zhu Y (2014) Structural characteristics of coal vitrinite during pyrolysis. Energy Fuels 28(6):3645–3654
34. Li M, Zeng F, Chang H, Xu B, Wang W (2013) Aggregate structure evolution of low-rank coals during pyrolysis by in-situ X-ray diffraction. Int J Coal Geol 116:262–269